Hypervirulent mutant of *Mycobacterium tuberculosis* resulting from disruption of the *mce1* operon

Nobuyuki Shimono*†‡, Lisa Morici*‡, Nicola Casali*, Sally Cantrell*, Ben Sidders*, Sabine Ehrt§, and Lee W. Riley*¶

*Division of Infectious Diseases, School of Public Health, University of California, Berkeley, CA 94720; †Medicine and Biosystemic Science, Kyushu University Graduate School of Medical Sciences, Fukuoka 812-8582, Japan; and §Department of Microbiology and Immunology, Weill Medical College of Cornell University, 1300 York Avenue, New York, NY 10021

Edited by John J. Mekalanos, Harvard Medical School, Boston, MA, and approved October 9, 2003 (received for review June 23, 2003)

An estimated one-third of the world's population is latently infected with *Mycobacterium tuberculosis*, the etiologic agent of tuberculosis. Here, we demonstrate that, unlike wild-type *M. tuberculosis*, a strain of *M. tuberculosis* disrupted in the *mce1* operon was unable to enter a stable persistent state of infection in mouse lungs. Instead, the mutant continued to replicate and killed the mice more rapidly than did the wild-type strain. Histological examination of mouse lungs infected with the mutant strain revealed diffusely organized granulomas with aberrant inflammatory cell migration. Murine macrophages infected *ex vivo* with the mutant strain were reduced in their ability to produce tumor necrosis factor α, IL-6, monocyte chemoattractant protein 1, and nitric oxide (NO), but not IL-4. The *mce1* mutant strain complemented with the *mce1* genes stimulated tumor necrosis factor α and NO production by murine macrophages at levels stimulated by the wild-type strain. These observations indicate that the *mce1* operon mutant is unable to stimulate T helper 1-type immunity in mice. The hypervirulence of the mutant strain may have resulted from its inability to stimulate a proinflammatory response that would otherwise induce organized granuloma formation and control the infection without killing the organism. The *mce1* operon of *M. tuberculosis* may be involved in modulating the host inflammatory response in such a way that the bacterium can enter a persistent state without being eliminated or causing disease in the host.

Approximately 60% of people who become infected with *Mycobacterium tuberculosis* develop asymptomatic latent infection (1). This reservoir of latently infected individuals has a 2–23% lifetime risk of developing active disease, referred to as reactivation tuberculosis (1). How *M. tuberculosis* establishes and maintains latent infection in an animal host is poorly understood. Several candidate *M. tuberculosis* genes have been recently reported to be important for persistence in the mouse model of tuberculosis. They include the isocitrate lyase gene (*icl*), mycolic acid cyclopropane synthase gene (*pca*), and a two-component response regulator called *mprA* (2–4). In each case, the disruption of the gene led to attenuation of the mutant strains in the mouse model of infection, whereas their *in vitro* growth kinetics remained similar to that of the respective wild-type strain (2–4).

We reported previously the identification of a *M. tuberculosis* gene *mce1A* (Rv0169, Sanger Centre genome sequence designation) that conferred on a nonpathogenic *Escherichia coli* strain an ability to enter nonphagocytic cells (5). The encoded product facilitated uptake of synthetic microspheres into nonphagocytic cells, and an active domain of the protein was recently shown to cause cytoskeletal rearrangement in HeLa cells that was both microfilament- and microtubule-dependent (6, 7). The gene *mce1A* is located in a putative operon called *mce1* containing 12 genes in the *M. tuberculosis* H37Rv genome (8) (Fig. 1*A*). The genome of *M. tuberculosis* contains four *mce* operons (*mce1–4*), each with a similar arrangement of the genes within the operon (8). Six of the *mce1* genes (*mce1A–F*) encode proteins with hydrophobic stretches at their N terminus, indicative of surface-exposed proteins. They were recently shown to localize to the cell wall fraction of *M. tuberculosis* (Fig. 9, which is published as supporting information on the PNAS web site), and Mce1A has been shown to be surface expressed (6).

The observed effect of the *mce1A* gene product on cytoskeletal rearrangement in HeLa cells and the presence of the Mce1 proteins in the mycobacterial cell wall suggest that the products of the *mce1* operon may affect the interaction of the pathogen with mammalian cells. We reasoned that in macrophages, the natural target of *M. tuberculosis*, such an interaction might alter host immune responses that determine the fate of both the organism and the host. In this report, we provide evidence that the *mce1* operon plays a major role in disease progression and outcome in mice infected with *M. tuberculosis*.

Materials and Methods

Disruption of the *mce1* Operon. First we disrupted *mce1A* (Rv0169) in *Mycobacterium bovis* bacillus Calmette–Guérin and *M. tuberculosis* (Erdman) strains by homologous recombination by using a previously described method (9). To disrupt *mce1A*, we cloned a 3.9-kb DNA fragment encompassing the *mce1A* gene into pBluescript (nonreplicative in mycobacteria) and replaced 1,040 bp of the *mce1A* gene with a *hyg* cassette conferring resistance to hygromycin. The resulting plasmid pMce:hyg was amplified in *E. coli* DH5α, and the sequence of the *mce1A* upstream and downstream region was confirmed. Five micrograms of pMce:hyg was pretreated with 100 mJ UV light cm^{-2} and electroporated into *M. tuberculosis* strain Erdman or bacillus Calmette–Guérin. The electroporated bacteria were kept in nonselective 7H9 medium with 10% ADC for 24 h and then plated onto 7H11 plates containing 10% oleic acid, albumin, dextrose, catalase, and 50 μg/ml hygromycin.

Next we disrupted another gene in the operon upstream of *mce1A* called *yrbE1B* (Rv0168) in *M. tuberculosis* strain H37Rv by using the two-step counter selection strategy described by Parish and Stoker (10). Briefly, the knockout vector was constructed by first inserting a hygromycin resistance cassette into p2NIL. Second, 2-kb regions upstream and downstream of Rv0168 were amplified from H37Rv DNA and cloned into the multicloning site flanking the hygromycin resistance gene. Finally, the *lacZ-sacB* counterselection cassette from pGOAL17 was inserted. Vector DNA was pretreated with 100 mJ UV light cm^{-2} and electroporated into *M. tuberculosis* strain H37Rv. Single crossovers were selected on 7H11 plates with 40 μg/ml 5-bromo-4-chloro-3-indolyl β-D-galactoside (X-Gal), 50 μg/ml hygromycin, and 20 μg/ml kanamycin. Double crossovers were selected on 7H11 plates containing 40 μg/ml X-Gal, 2% sucrose, and 50 μg/ml hygromycin. The candidate double crossover mutants were screened by PCR and then confirmed by Southern blot hybridization.

We performed immunoblot analyses of the Mce1 proteins using available antibodies and found that the *mce1A* and *yrbE1B* mutants

This paper was submitted directly (Track II) to the PNAS office.

Abbreviations: MCP-1, monocyte chemoattractant protein 1; cfu, colony-forming unit; TNFα, tumor necrosis factor α; moi, multiplicity of infection.

‡N.S. and L.M. contributed equally to this study.

¶To whom correspondence should be addressed. E-mail: lwriley@uclink4.berkeley.edu.

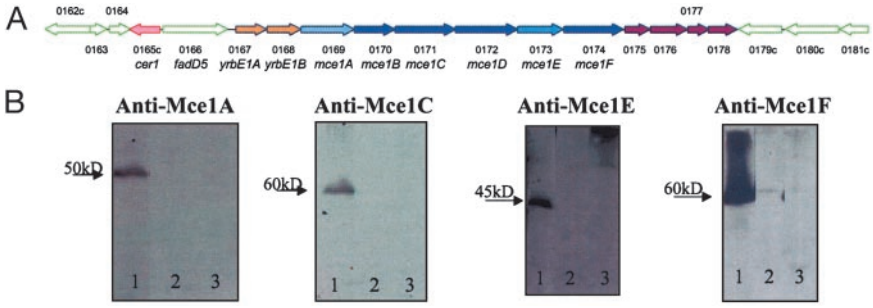

Fig. 1. (*A*) *mce1* operon based on *M. tuberculosis* H37Rv genome sequence (8). (*B*) Western blot analysis of wild-type *M. tuberculosis* H37Rv (lane 1) (Rv 0169), *yrbE1B* (Rv0168) H37Rv mutant (lane 2), and *mce1A* Erdman mutant (lane 3). The immunoblot analysis was performed with a rabbit polyclonal antibody raised against Mce1A, Mce1C, Mce1E, or Mce1F. The antibodies recognize the respective *mce1* operon proteins encoded by the wild-type strain only. Disruption of *yrbE1B* or *mce1A* by the hygromycin resistance gene cassette led to loss of expression of downstream genes in the operon.

did not express the products of *mce1A*, *C*, *E*, and *F* (Fig. 1*B*). Thus, allelic exchange of *mce1A* or *yrbE1B* led to the disruption of the downstream *mce1* genes. Henceforth, *mce1A* or *yrbE1B* mutants will be referred to as *mce1* operon mutants. All of these mutants showed *in vitro* broth (7H9) growth kinetics indistinguishable from that of the respective wild-type strains (data not shown). The studies described below were performed with the *mce1* operon mutants and their respective parent wild-type strains.

Complementation of the *mce1* Mutant Strain. Despite numerous attempts, it was not possible to complement the *mce1* operon knockout mutants by expression of the missing genes from an alternative locus or plasmids. Thus, we adopted a knockin strategy, whereby the disrupted genes were replaced at the original locus. The knockin vector contained a 5.6-kb fragment of the *mce1* operon encompassing Rv 0167–Rv 0171. In the first cloning step, the upstream 3.6-kb fragment containing a C-terminal 6× histidine (HIS) tag was cloned between *Hin*dIII and *Xba*I sites of p2NIL (10) (see Fig. 10, which is published as supporting information on the PNAS web site). In the second step, the remaining 2 kb was cloned between the *Xba*I and *Pac*I sites. Cloning the entire fragment in two steps allowed us to engineer the 6× HIS tag immediately preceding the stop codon for *mce1A* and the start codon for *mce1B*. The placement of a 6× HIS tag and an *Xba*I restriction site between *mce1A* and *mce1B* was confirmed by sequencing and used to distinguish the complemented from the wild-type strain. Last, a *lacZ-sacB* cassette was cloned into the *Pac*I site of p2NIL for two-step counter selection of knockin mutants (10). The Erdman and H37Rv *mce1* operon mutants were transformed with the knockin construct. Single crossovers were selected on 7H11 plates with 40 μg/ml 5-bromo-4-chloro-3-indolyl β-D-galactoside (X-Gal) and 20 μg/ml kanamycin. Double crossovers were selected on 7H11 plates with 40 μg/ml X-Gal and 2% sucrose.

The Erdman mutant strain could not be complemented, most likely due to poor transformation efficiency. Colonies representing potential double crossovers in H37Rv were screened by PCR, and knockin strains were confirmed by Southern blot analysis and sequencing. Expression of Mce1 proteins was demonstrated by Western blot analysis (see Fig. 11, which is published as supporting information on the PNAS web site).

Mouse Infection. *M. tuberculosis* H37Rv, Erdman, *M. bovis* bacillus Calmette–Guérin, and their mutant constructs were each passaged once in mice before use. They were grown in 7H9 broth for animal inoculation or 7H11 agar for colony-forming unit (cfu) enumeration.

We infected 8-wk-old female BALB/c mice (The Jackson Laboratory) via tail vein with 0.1 ml of PBS, pH 7, suspension containing $\approx 3 \times 10^5$ cfu of the wild-type or *mce1* mutant bacillus Calmette–Guérin or 3.5×10^5 cfu of the wild-type or *mce1* mutant *M. tuberculosis* Erdman. Each infection group included 42–50 animals. At regular intervals (2, 4, 10, 16, 25, and 41 wk), four animals from each group were killed and lungs, spleen, and liver were removed and examined grossly, histologically, and microbiologically. Histology slides were made commercially, and they were examined by a veterinary pathologist specializing in mouse pathology. We enumerated bacterial recovery from each organ by comparing cfu on 7H11 agar plates.

Murine Macrophage Infections. Peritoneal exudate cells were obtained from an uninfected mouse peritoneal cavity washed with 8 ml of Hanks' balanced saline solution (HBSS) 3 days after the administration of 2 ml of 3% thioglycolate (Difco). The cells were suspended at a concentration of 5×10^5 cells per ml in culture medium consisting of RPMI medium 1640 supplemented with 10% FCS and 100 μg/ml ampicillin. They were cultured in 24-well plates overnight at 37°C. Nonadherent cells were then removed by gentle washing with warm HBSS, and adherent cells were used as macrophages. Macrophages were infected with wild-type bacillus Calmette–Guérin (3.5×10^5 cfu/ml) or *mce1* mutant bacillus Calmette–Guérin (1.8×10^6 cfu/ml), wild-type Erdman (7.5×10^5 cfu/ml) or *mce1* mutant Erdman (1.5×10^6 cfu/ml), wild-type H37Rv (1×10^6 cfu/ml) or *mce1* mutant H37Rv (1.5×10^6 cfu/ml), or PBS alone for 24 h. The culture supernatant of macrophages was collected, filtered through a 0.2-μM pore membrane, and stored at –80°C until analysis. Tumor necrosis factor α (TNFα) levels were measured by ELISA (R & D Systems).

Kinetic analyses were performed with RAW 264.7 murine macrophage-like cell line (American Type Culture Collection), which was cultured and maintained in DMEM (GIBCO) supplemented with 10% FBS (Omega Scientific, Tarzana, CA) and 1% penicillin/streptomycin (BioWhittaker) in a 5% CO_2 humidified incubator at 37°C. Cells were plated at 1×10^5 cells per ml in 24-well tissue culture plates and incubated overnight until they were $\approx$70% confluent. Viability of cells was monitored for all experimental conditions by trypan blue exclusion. In addition, culture supernatants were harvested, and cell death was assessed by the lactate dehydrogenase-release assay (Roche, Gipf-Oberfrick, Switzerland).

We incubated 10^4 or 10^5 bacteria with 10^5 RAW macrophages in triplicate wells of a 24-well plate for a multiplicity of infection (moi) of 1:10 or 1:1, respectively. After 2 h of infection, macrophages were washed three times with DMEM to remove extracellular bacteria. Lipopolysaccharide (1 μg/ml) (Sigma) was used as a positive control, and uninfected or mock-infected (PBS) macrophages served as negative controls for each experiment. For some experiments, RAW macrophages were activated with 30 units/ml recombinant IFN-γ (R & D Systems) 24 h before infection. At least three independent experiments were performed for each strain, and macrophages were infected in triplicate for each experiment. For some of the cytokines, we repeated the infections with primary murine bone marrow macrophages to confirm our observations with RAW cells.

TNFα, IL-4, IL-6, and monocyte chemoattractant protein 1 (MCP-1) produced by RAW macrophages in response to infection with the *M. tuberculosis* strains were measured by ELISA (R & D Systems). The amount of nitric oxide (NO) produced by macro-

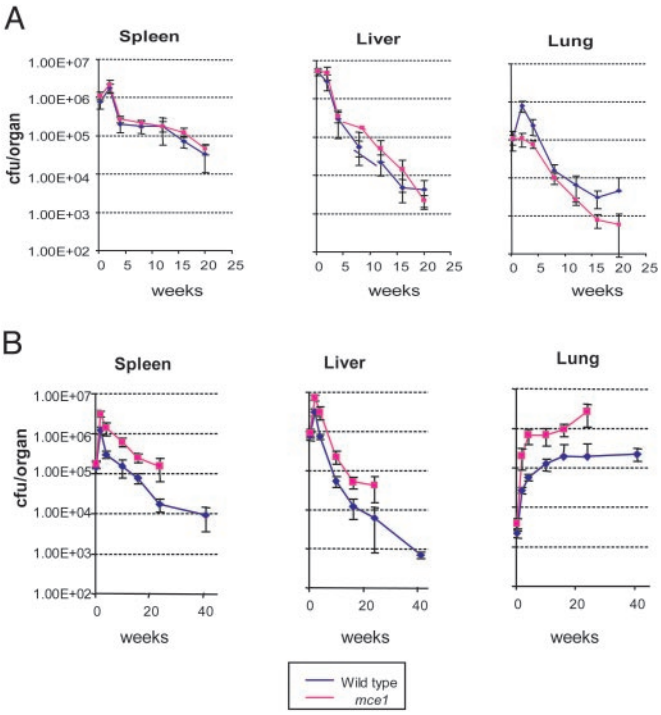

Fig. 2. Time course of infection after tail vein injection of bacillus Calmette–Guérin wild-type and *mce1* mutant (*A*) and *M. tuberculosis* Erdman wild-type and *mce1* mutant (*B*). Recovery of the bacteria is enumerated by cfu per organ at 0, 2, 4, 10, 16, 25, and 41 wk after injection. The curve for cfu recovered from mice infected with the *M. tuberculosis mce1* mutant stops at ≈27 wk, because all of the initially infected mice were dead by this time point.

phages in each experimental infection was assessed in culture supernatant by the Griess colorimetric assay (Promega).

Murine bone marrow macrophages were plated at 5×10^5 cells per well in 24-well plates and incubated overnight. The next day, 300 units of IFN-γ was added to each well, and 24 h later, mycobacteria were added at a moi of 1:1. TNFα and NO levels were measured 24 h after infection.

To control for the effect of potential differences in the number of bacterial organisms interacting with macrophages, we compared intracellular uptake or survival of the organisms by lysing macrophages with 200 μl of PBS/0.1% Triton X-100 and plating serial dilutions on 7H11 agar to enumerate cfu. This was performed at 2 h postinfection (day 0) through day 4. cfu were enumerated after 3–4 wk of plate incubation.

Statistics. Data are presented from representative experiments as the mean ± SE of triplicate infections. Differences between the means of each treatment group were analyzed by Student's *t* test and were considered significant at $P < 0.05$.

Results

Mouse Virulence Studies. No difference in bacterial cfu recovery from spleen or liver was observed at any time point in mice infected with wild-type or mutant bacillus Calmette–Guérin (Fig. 2*A*). However, the number of cfu recovered from lungs of mice infected with wild-type bacillus Calmette–Guérin was significantly higher than that recovered from lungs of mice infected with the *mce1* mutant bacillus Calmette–Guérin, especially after 20 wk of infection (Fig. 2*A*). Unexpectedly, in mice infected with *M. tuberculosis*, the number of cfu recovered even after 2 wk of infection from each of the organs was significantly greater for mice infected with the *mce1* mutant strain compared with that in mice infected with the wild-type strain (Fig. 2*B*). Most importantly, in the lungs, the cfu

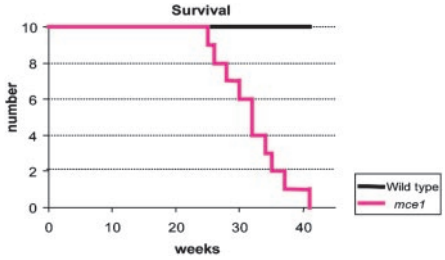

Fig. 3. Survival kinetics of BALB/c mice infected with *M. tuberculosis* Erdman. Ten mice each were initially infected via tail vein and followed for the indicated number of weeks. By 41 wk, all mice infected with the *mce1* mutant strain were dead.

continued to increase over time in mice infected with the *mce1* mutant Erdman strain until the animals died, whereas in mice infected with the wild-type Erdman strain, the number of recovered organisms reached a plateau after ≈17 wk and remained unchanged up to 41 wk of follow-up (Fig. 2*B*). The mutant-infected mice started to die as early as 27 wk after infection, and by 41 wk, 100% of a group of 10 initially infected mice were dead, whereas all 10 of the wild-type-infected mice remained alive at 41 wk (Fig. 3).

Mouse Pathology Studies. Gross organ examinations revealed that as early as 16 wk after infection, the lung surface of mice infected with the wild-type bacillus Calmette–Guérin showed a greatly increased number (>500) of discrete well-circumscribed granulomas (Fig. 4*Aa*) compared with the lungs of mutant-infected mice (<20) (Fig. 4*Ab*). In Erdman *M. tuberculosis*-infected mice, the lungs infected with the wild-type strain showed progressively enlarging granulomas with sharp circumscribed borders (Fig. 4*Ac*), whereas the lungs of mutant-infected mice showed progressively enlarging granulomas that were diffuse, poorly circumscribed, and coalescing (Fig. 4*Ad*). Differences in the gross pathology changes between the Erdman mutant and wild-type-infected mice were evident as early as 10 wk of infection.

Histologic examination revealed that around 12 wk, the lungs of mice infected with the mutant bacillus Calmette–Guérin were typically characterized by granulomatous pneumonia with multifocal small granulomas consisting of macrophages containing eosinophilic cytoplasm, and occasional granulomas consisting of epithelioid binucleated macrophages with peripheral infiltrate of lymphocytes and plasma cells (Fig. 4*Bb*). In the wild-type bacillus Calmette–Guérin-infected mice, there was moderate to severe granulomatous pneumonia characterized by multiple foci of granulomas of varying degrees of severity (Fig. 4*Ba*). At 16 wk, lungs of mice infected with the wild-type Erdman strain contained a higher density of lymphocytes and fewer coalescent granulomas (Fig. 4*Bc*), whereas lungs infected with the mutant Erdman strain contained large epithelioid granulomas with intralesional cholesterol clefts and lymphocytic and plasma cell infiltration affecting 25–50% of the lung parenchyma (Fig. 4*Bd*).

In bacillus Calmette–Guérin-infected mice, despite nonsignificant differences between wild-type and mutant strain-infected mice in the number of cfu recovered from lungs up to 15 wk, there were dramatic gross and histologic differences in the number and size of granulomatous lesions detected. Although it is difficult to attribute the differences in the extent of lung pathology in Erdman-infected mice to the number of organisms present in the lungs vs. the effect of *mce1* products, the observation we made with bacillus Calmette–Guérin-infected mice, controlling for the number of organisms recovered, suggests that the absence of *mce1* expression contributes to an aberrant host cell response that leads to less well-organized granuloma formation.

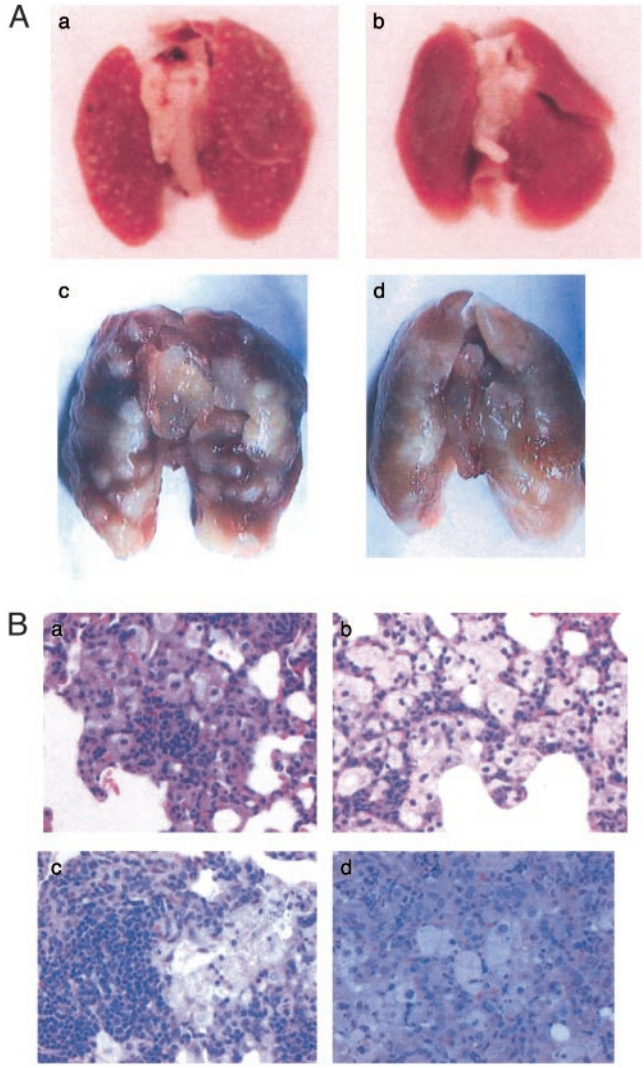

Fig. 4. (*A*) Gross examination of lungs of BALB/c mice infected with bacillus Calmette–Guérin or *M. tuberculosis*. Lungs of mice were examined after 16 wk of infection with the wild-type bacillus Calmette–Guérin (*a*) or bacillus Calmette–Guérin *mce1* mutant (*b*). Lungs of mice were examined after 32 wk of infection with wild-type *M. tuberculosis* Erdman (*c*) or *M. tuberculosis* Erdman *mce1* mutant (*d*). Lung lesions with discrete well circumscribed borders are evident in wild-type-infected lungs, whereas lungs infected with either of the *mce1* mutants show coalescing poorly circumscribed lesions. (*B*) Histological examination (hematoxylin/eosin stain) of lung sections of BALB/c mice infected with bacillus Calmette–Guérin or *M. tuberculosis* Erdman. At 12 wk of infection, there is greater and denser lymphocyte infiltration in lungs infected with the wild-type bacillus Calmette–Guérin strain (*a*), whereas the lungs infected with the mutant bacillus Calmette–Guérin show many foamy macrophages with sparse migration of lymphocytes (*b*). At 16 wk of infection with *M. tuberculosis*, lungs infected with the wild-type strain show densely packed lymphocytes surrounded by macrophages (*c*), whereas lungs infected with the mutant strain show mostly macrophages with diffuse distribution of the lymphocyte population (*d*). (Magnification in *B*, ×400.)

Cytokine Production by Infected Murine Macrophages. Because TNFα is essential for granuloma formation (11, 12), we analyzed TNFα production by thioglycolate-stimulated murine peritoneal macrophages infected *ex vivo* with bacillus Calmette–Guérin, Erdman, or H37Rv. The levels of TNFα expression as measured by ELISA were significantly less in cells infected with the bacillus Calmette–Guérin, Erdman, or H37Rv *mce1* operon mutant strains compared with those infected with the respective wild-type strains (Fig. 5).

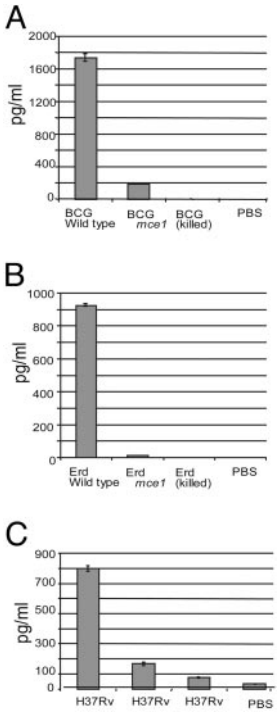

Fig. 5. TNFα determinations in BALB/c peritoneal macrophages infected *ex vivo* with bacillus Calmette–Guérin or *M. tuberculosis*. TNFα levels were measured in cells infected with live bacillus Calmette–Guérin wild-type or *mce1* mutant (*A*), *M. tuberculosis* Erdman or *mce1* mutant (*B*), and *M. tuberculosis* wild-type H37Rv or *mce1* mutant (*C*). Control cells were mock-infected with PBS in each experiment.

To further characterize the interaction of *mce1* mutants with macrophages, we performed kinetic studies with RAW macrophages. Similar to the observation made with peritoneal macrophages, RAW macrophages infected with H37Rv *mce1* mutant produced ≈4- to 6-fold less TNFα than macrophages infected with wild-type H37Rv after 24 h of infection. ($P < 0.05$) (Fig. 6*A*). The H37Rv *mce1* mutant was significantly reduced in its ability to stimulate early TNFα production ($P < 0.05$) (8 h postinfection), and by 72 h postinfection, the H37Rv *mce1* mutant still failed to elicit significant TNFα production (Fig. 6*A*).

In addition to a defect in TNFα production, RAW macrophages infected with H37Rv *mce1* mutant produced very little IL-6 or MCP-1 over a 72-h period (Fig. 6 *B* and *C*). IL-6 production peaked at 72 h for H37Rv wild-type-infected RAW cells, reaching >2,000 pg/ml. However, cells infected with H37Rv *mce1* mutant produced levels of IL-6 equivalent to that of uninfected cells (<100 pg/ml) (Fig. 6*B*). After 24 h, RAW macrophages produced ≈11-fold less MCP-1 when infected with H37Rv *mce1* mutant compared with the cells infected with wild-type H37Rv. MCP-1 expression by H37Rv wild-type-infected cells peaked at 48 h postinfection to >30,000 pg/ml, whereas the *mce1* mutant-infected cells produced significantly less MCP-1 (3,000 pg/ml) ($P < 0.05$) (Fig. 6*C*). IL-4 expression was measured in RAW cells infected for 24 h for comparison. IL-4 was produced by RAW cells at detectable levels but showed no significant difference between cells infected with the Erdman *mce1* mutant (80 pg/ml, SE 6.9) or the wild-type (74 pg/ml, SE 4.8) strain ($P > 0.05$).

NO Production and Intracellular Growth. We also measured the kinetics of NO production in infected RAW macrophages up to 72 h. Over the course of the infection, H37Rv *mce1* stimulated significantly less nitrite production than did H37Rv wild type ($P < 0.05$, Fig. 7*A*). NO production by RAW macrophages in

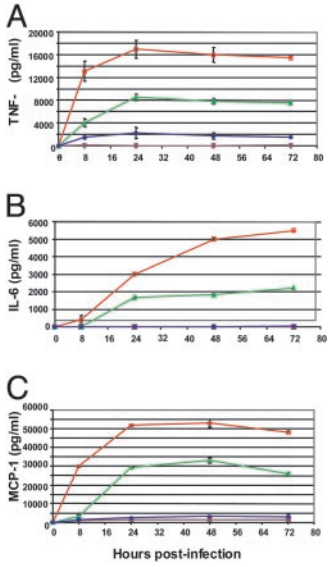

Fig. 6. Kinetic analysis of TNFα (*A*), IL-6 (*B*), and MCP-1 (*C*) production by RAW macrophages infected with H37Rv wild-type (green) or *mce1* mutant (blue) strains at a moi of 1:1. Controls included uninfected RAW cells (maroon) or lipopolysaccharide-treated cells (red).

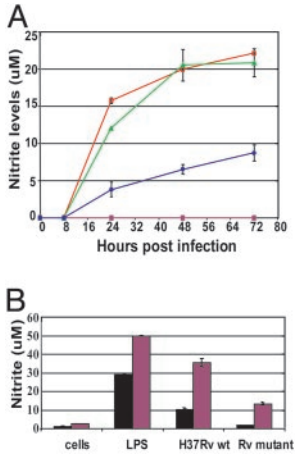

Fig. 7. (*A*) Kinetic analysis of nitrite production by RAW macrophages infected with H37Rv wild-type (green) or *mce1* mutant (blue) strains at a moi of 1:1. Controls included uninfected RAWs (solid squares) or lipopolysaccharide-treated cells (red). (*B*) Nitrite production by untreated (black bar) and IFN-γ-pretreated (maroon bar) RAW macrophages infected with H37Rv wild-type or *mce1* mutant strains (moi 1:1) 24 h after infection.

response to infection with H37Rv *mce1* was 3- to 4-fold less than that stimulated by H37Rv wild type after 24 h of infection. Moreover, by 72 h postinfection, the *mce1* mutant failed to induce NO at levels induced by wild-type H37Rv as early as 24 h postinfection. Similar differences in NO production were also observed between Erdman wild-type and Erdman *mce1* mutant-infected macrophages (data not shown).

When equal cfu for each strain were added to macrophages, there was no significant difference in the number of bacteria recovered ($2.1–3.9 \times 10^4$ cfu/ml) from infected RAW cells 2 h postinfection, indicating that there were no differences in the ability of the strains to invade RAW macrophages (see graphs in Fig. 12*A*, which is published as supporting information on the PNAS web site). However, after 2 days of infection, there was a greater number of bacteria recovered from cells infected with H37Rv *mce1* mutant (1.3×10^5 cfu/ml) than cells infected with H37Rv wild type (2.5×10^4 cfu/ml) ($P < 0.05$). The *mce1* mutant continued to proliferate up to day 4, at which time the experiment was terminated due to decreased cell viability. In contrast to the *mce1* mutant, the cfu recovered from the wild-type-infected cells remained constant ($2 - 2.5 \times 10^4$ cfu/ml) over 4 days, although after 4 days, the cfu recovery of the wild-type strain increased. This difference in intracellular proliferation was also observed when RAW cells were infected with the Erdman wild-type and *mce1* mutant strains (data not shown).

Because macrophages infected with the *mce1* mutant strains produced significantly less NO than wild-type-infected cells, and because NO has been shown to be bacteriostatic to *M. tuberculosis in vitro*, we tested whether pretreatment of the macrophages with IFN-γ could enhance the NO production of macrophages infected with the *mce1* mutant and thus inhibit its intracellular growth. Pretreatment of macrophages with IFN-γ did increase the nitrite levels of H37Rv *mce1* mutant-infected RAW cells to that of wild-type-infected RAW cells (but the levels were still significantly reduced compared with wild-type-infected RAW cells also pretreated with IFN-γ) (Fig. 7*B*). Treatment of the RAW cells with IFN-γ enabled the macrophages to suppress the growth of the *mce1* mutant strain intracellularly (see Fig. 12*B*).

Coinfection with H37Rv Wild-Type and *mce1* Mutant Strains. To test whether the *mce1* mutant strain directly inhibited macrophage activation rather than failed to induce the macrophage's response to infection, we coinfected RAW cells with the H37Rv wild-type and H37Rv *mce1* strains at a moi of 2:1. Coinfected macrophages produced TNFα ($9{,}600 \pm 910$ pg/ml) and NO levels (11.9 ± 0.6 μM) equal to that induced by infection with wild-type H37Rv alone ($8{,}840 \pm 642$ pg/ml and 11.1 ± 0.7 μM, respectively). Furthermore, growth and survival of each strain were determined on 7H11 plates with and without 40 μg/ml hygromycin at days 0, 2, and 4. In coinfected macrophages, a similar number of cfu ($2–3.8 \times 10^4$ cfu/ml) were recovered for each strain over the infection period, and no growth was observed, suggesting that the activated response of the macrophage to the wild-type strain was sufficient to inhibit the growth of the *mce1* mutant strain (Fig. 12*C*). However, it should be noted that the possible suppressive effect of the mutant strain, even if it had such an effect, may not have been detectable at the moi used in this experiment.

Complementation of the H37Rv *mce1* Mutant. IFN-γ-stimulated bone marrow macrophages derived from the femurs of 6- to 8-wk-old BALB/c mice were infected with 1×10^5 H37Rv wild-type, *mce1* mutant, or the complemented *M. tuberculosis* H37Rv strain. The levels of TNFα and NO production by macrophages infected with the complemented strain were equivalent to that observed with the wild-type strain, supporting the causal role of the *mce1* operon products in the observed phenotype of the mutant (Fig. 8).

Discussion

The disruption of the *mce1* operon in *M. tuberculosis* led to hypervirulence of the mutant strain and aberrant granuloma formation in mice. Furthermore, murine macrophages infected *ex vivo* with the *mce1* mutant strains, compared with the corresponding wild-type strains, were reduced in their ability to express TNFα, IL-6, MCP-1, and NO, but not IL-4. The *mce1* mutant complemented with the *mce1* operon genes was restored in its ability to induce the proinflammatory response by the macrophages. These observations are consistent with the suggestion that the *mce1* operon products are associated with the induction of a proinflammatory response or T helper 1-type immunity in mice.

In the mouse infection, we observed that *M. tuberculosis* and *M. bovis* bacillus Calmette–Guérin disrupted in the *mce1* operon failed to elicit well organized granuloma formation. Lungs of *M. tuberculosis* wild-type and bacillus Calmette–Guérin wild-type-infected

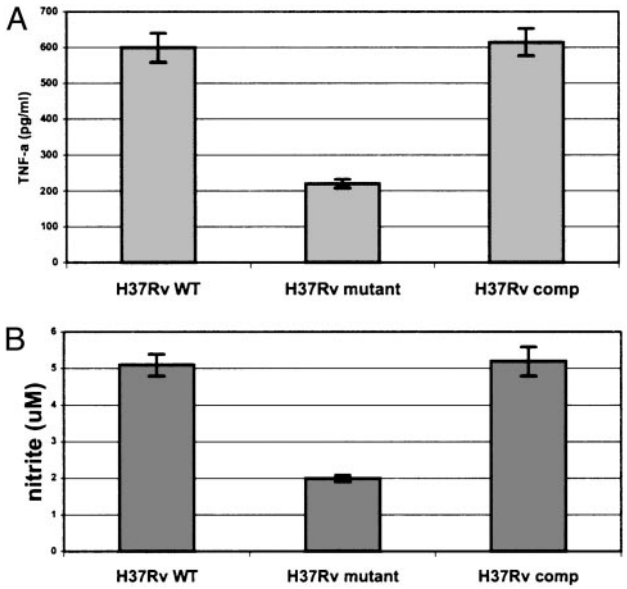

Fig. 8. TNFα (*A*) and nitrite (*B*) production by IFN-γ-treated murine bone marrow-derived macrophages infected with H37Rv wild-type, mutant, or *mce1* operon-complemented strain of *M. tuberculosis*. The cells were infected with 1×10^5 bacilli at a moi of 1:10, and the TNFα or nitrite measurements were made at 24 h of infection. Each bar represents a mean value $\pm$ SD of infection done in triplicate per strain.

mice showed numerous well organized granulomas that appeared to be associated with control of the proliferation of the bacilli, as evidenced by the plateau in the cfu recovery curve after 15–17 wk of infection (Fig. 2*B*). In contrast, the absence of organized granulomas in the *M. tuberculosis mce1* mutant-infected mice was associated with a significantly greater number of bacilli in the lungs, which eventually killed the mice (Figs. 2*B* and 3). The observed granuloma formation in mice infected with the *mce1*-disrupted *M. tuberculosis* or bacillus Calmette–Guérin strains resembles that observed in TNFα-deficient mice infected with *M. tuberculosis* (13–17). These observations suggest that a certain level of proinflammatory response is necessary for *M. tuberculosis* to establish a stable nonproliferative state of infection in the animal.

The observed differences in proinflammatory response could be related to the differences in the number of intracellular organisms. However, the results from the *in vivo* study with bacillus Calmette–Guérin-infected mice as well as the *ex vivo* macrophage infection studies that controlled for the number of recovered organisms show that the proinflammatory cellular and cytokine responses depend more on the presence of the *mce1* operon in the infecting strain than the differences in the number of organisms. That is, the diminished proinflammatory response appears to allow the enhanced proliferation of the intracellular mutant strain.

At this time, we do not know which product or set of products of the *mce1* operon mediates the hypervirulence and macrophage cytokine expression patterns we describe above. The complemented strain was able to stimulate TNFα and NO expression in murine macrophages *in vitro*, which provides evidence for the causal role of the operon in the induction of a T helper 1-type immune response. Furthermore, we found that all of the independent *mce1* mutants (bacillus Calmette–Guérin *mce1A*, *M. tuberculosis* Erdman *mce1A*, and *M. tuberculosis* H37Rv *yrbE1B*) we have constructed yielded the same pattern of cytokine response by the mouse macrophages. The disruption of cell wall proteins encoded by some of the *mce1* genes (*mceA–F*) may alter the structure of nonprotein cell wall components, which in turn may have an immunomodulatory effect. Or, the Mce1 proteins themselves may form a complex in the cell wall that transports products extracellularly that have a proinflammatory effect. One of the *mce1* proteins (Mce1E) is a putative lipoprotein, which may induce proinflammatory responses by macrophages via toll-like receptor 2 (18, 19).

Manca *et al.* (20) recently examined the differential response of mice to infection by using clinical *M. tuberculosis* isolates (20). One isolate HN878 was found to be hypervirulent in mice, and they found that this phenotype was associated with 2- to 4-fold lower levels of TNFα, IL-6, IL12, and IFNγ mRNA in lungs of mice infected with this strain (20). They suggested that the hypervirulence of this strain may be due to failure of the strain to stimulate T helper 1 type immunity (20). Our findings are consistent with this view and raise an intriguing possibility that the different clinical manifestations, latent infection, rapidly progressive disease, and reactivation tuberculosis, after *M. tuberculosis* infection may be influenced by a regulated expression of the Mce products.

Hypervirulence has recently been reported with another human intracellular pathogen, *Leishmania major* (21). Cunningham *et al.* (21) reported that *L. major* disrupted in pteridine reductase 1 express low levels of tetrahydrobiopterin, which is needed to control differentiation of the parasite into the metacyclic promastigote. Such mutants were arrested in the amastigote stage, were highly infectious to mice, and produced larger cutaneous lesions. More recently, four *M. tuberculosis* strains with mutations in distinct two-component regulatory system genes were shown to become hypervirulent in the SCID mouse model, suggesting that *M. tuberculosis* has a set of genes that enables the organism to keep its *in vivo* proliferation in check even in an immunocompromised animal (22). These observations suggest that the disruption of genes of pathogens associated with persistent infection may unmask the organism's full virulence potential. The *M. tuberculosis mce1* operon may have evolved to "fine-tune" the host immune response to the bacillus' advantage to establish latent infection without causing active disease in the host.

We thank Ryan Senaratne, Takao Fujimura, and Marvin Ryou for assistance with the animal studies and gene disruption experiments. This work was supported by a grant from National Institute of Allergy and Infectious Diseases, National Institutes of Health (AI35266).

1. Parrish, N. M., Dick, J. D. & Bishai, W. R. (1998) *Trends Microbiol.* **6,** 107–112.
2. Mckinney, J. D., zu Bentrup, D. H., Munoz-Elias, E. J., Miczak, A. Cehn, B., Chan, W., Swenson, D., Sacchettini, J. C., Jacobs, W. R. & Russell, D. G. (2000) *Nature* **406,** 735–738.
3. Glickman, M. S., Cox, J. S. & Jacobs, W. R. (2000) *Mol. Cell* **5,** 717–727.
4. Zahrt, T. C. & Deretic, V. (2001) *Proc. Natl. Acad. Sci. USA* **98,** 12706–12711.
5. Arruda, S., Bomfim, G., Knights, R., Huima-Byron, T. & Riley, L. W. (1993) *Science* **261,** 1454–1457.
6. Chitale, S., Ehrt, S., Kawamura, I., Fujimura, Y., Shimono, N., Anand, N., Lu, S., Cohen-Gould & L. Riley, L. W. (2001) *Cell Microbiol.* **3,** 247–254.
7. Casali, N., Konieczny, M., Schmidt, M. A. & Riley, L. W. (2002) *Infect. Immun.* **70,** 6846–6852.
8. Cole, S. T., Brosch, R., Parkhill, J., Garnier, T., Churcher, C., Harris, D., Gordon, S. V., Eiglmeier, K., Gas, S., Barry, C. E., III, *et al.* (1998) *Nature.* **393,** 537–544.
9. Hinds, J., Mahenthiralingam, E., Kempsell, K. E., Duncan, K., Stokes, R. W., Parish, T. & Stoker, N. G. (1999) *Microbiology* **145,** 519–527.
10. Parish, T. & Stoker, N. G. (2000) *Microbiology* **146,** 1969–1975.
11. Saunders, B. M. & Cooper, A. M. (2000) *Immunol. Cell. Biol.* **78,** 334–341.
12. Orme, I. M. & Cooper, A. M. (1999) *Immunol. Today* **20,** 307–312.
13. Kindler, V., Sappino, A., Grau, G., Piguet, P. & Vassalli, P. (1989) *Cell* **56,** 731–740.
14. Flynn, J. L., Goldstein, M. M., Chan, J., Triebold, K. J., Pfeffer, K., Lowenstein, C. J., Schreiber, R., Mak, T. W. & Bloom, B. R. (1995) *Immunity* **2,** 561–572.
15. Senaldi, G., Yin, S., Shaklee, C. L., Piguet, P.-F., Mak, T. W. & Ulich, T. R. (1996) *J. Immunol.* **157,** 5022–5026.
16. Bean, A. G., Roach, D. R., Briscoe, H., France, M. P., Korner, H., Sedgwick, J. D. & Britton, W. (1999) *J. Immunol.* **162,** 3504–3511.
17. Mohan, V. P., Scanga, C. A., Yu, K., Scott, H. M., Tanaka, K. E., Tsang, E., Tsai, M. C., Flynn, J. L. & Chan, J. (2001) *Infect. Immun.* **69,** 1847–1855.
18. Underhill, D., Ozinsky, A., Smith, K. & Aderem, A. (1999) *Proc. Natl. Acad. Sci. USA* **96,** 14459–14463.
19. Brightbill, H., Libraty, D., Drutzik, S., Yang, R., Belisle, J., Bleharski, J., Maitland, M., Norgard, M., Plevy, S., Smale, S., *et al.* (1999) *Science.* **285,** 732–735.
20. Manca, C., Tsenova, L., Begtold, A., Freeman, S., Tovey, M., Musser, J. M., Barry, C. E., III., Freedman, V. H. & Kaplan, G. (2001). *Proc. Natl. Acad. Sci. USA* **98,** 5752–5757.
21. Cunningham, M. L., Titus, R. G., Turco, S. J. & Beverley, S. M. (2001) *Science* **292,** 285–287.
22. Parish, T., Smith, D. A. Kendall, S., Casali, N., Bancroft, G. J. & Stoker, N. G. (2003) *Infect. Immun.* **71,** 1134–1140.